Electronic structure of the CdKr lowest Rydberg state determined from laser-excitation spectra using supersonic beam and double optical resonance methods

J. Koperski[1,*] and M. Czajkowski[2,†]

[1]*Instytut Fizyki, Uniwersytet Jagielloński, Reymonta 4, 30-059 Kraków, Poland*
[2]*Department of Physics, University of Windsor, Windsor, Ontario, Canada N9B3P4*
(Received 8 October 2003; revised manuscript received 8 January 2004; published 14 April 2004)

The lowest $E\,^3\Sigma^+(6\,^3S_1)$ Rydberg state of the CdKr van der Waals complex was investigated using supersonic-expansion beam and the optical-optical double-resonance methods. Well-defined vibrational levels $A\,^3 0^+_{v''=9}(^3\Pi)$ and $B\,^3 1^+_{v''=1}(^3\Sigma^+)$ were used as intermediate states being excited from the $X\,^1 0^+(^1\Sigma^+)$ ground state. Two types of bound-bound excitation spectra of the $E\,^3\Sigma^+ \leftarrow A\,^3 0^+$ and $E\,^3\Sigma^+ \leftarrow B\,^3 1$ transitions were observed and recorded. The analyses of the spectra suggest an existence of two, well-defined minima in the $E\,^3\Sigma^+$-state potential-energy (PE) curve: an inner PE well E_1 with $D'_e(E_1) = 1656$ cm^{-1} and an outer well E_2 with $D'_e(E_2) = 27$ cm^{-1}, separated from each other by a positive-energy barrier. Combination of bound-bound spectra excited from different intermediate states enabled probing of the $E\,^3\Sigma^+$-state potential in a relatively large range of internuclear separations R and hence it led to a complete determination of spectroscopical parameters of the $E\,^3\Sigma^+$-state PE curve. The height of the barrier and its approximate location were also determined. The experimental results of this investigation coincide well with the results of *ab initio* calculation of Czuchaj and co-workers [Chem. Phys. **248**, 1 (1999); Theor. Chem. Acc. **105**, 219 (2001)].

I. INTRODUCTION

In recent papers by Czuchaj and Stoll [1] and Czuchaj *et al.* [2,3], the authors report on results of *ab initio* calculation on CdRG and HgRG (RG=rare gas atom) van der Waals (vdW) complexes. They obtained potential-energy (PE) curves and spectroscopic parameters of the molecular ground and several excited states including $^3\Sigma^+$ and $^1\Sigma^+$, the lowest Rydberg states asymptotically correlating with the n^3S_1 and n^1S_0 [Cd $(n \geqslant 6)$, Hg $(n \geqslant 7)$] atomic asymptotes, respectively. Theoretical predictions regarding the excited-state potentials are in great demand among the members of the community of experimental spectroscopy. Czuchaj and co-workers [1–3] seem to fulfill these demands with respect to the diatomic clusters mentioned above. They have clearly shown that their *ab initio* calculated Rydberg-state PE curves of CdHe and HgHe are entirely repulsive. However, in case of CdNe and HgNe complexes the curves should display well-defined energy barriers (as they call them humps), while approaching smaller internuclear separation values R. Interestingly, these barriers transform into shallow minima at yet shorter values of R, while the whole PE curve lies entirely above the dissociation limit correlating with the atomic asymptotes. The success of the *ab initio* results becomes quite evident if a total agreement of theoretical predictions with experimental laser-spectroscopy findings [4–6] is mentioned. In the very recent papers on CdNe and CdAr vdW complexes in their lowest $E\,^3\Sigma^+(6\,^3S_1)$ Rydberg state, Koperski and Czajkowski [5,6] corroborated qualitatively, and to great extent quantitatively, theoretical results of Refs. [1,2]. The experiments were based on the optical-optical double-

resonance (OODR) method using two intermediate states $A\,^3 0^+(^3\Pi)$ and $B\,^3 1(^3\Sigma^+)$ to explore the structure of the $E\,^3\Sigma^+$-state PE curve in relatively large interval values of R. Earlier, in a similar way Okunishi and co-workers [4,7] investigated the HgNe and HgAr complexes in the $^3\Sigma^+$ molecular state which asymptotically correlates with the $7\,^3S_1$ Hg atomic level. Though their experimental results were obtained prior to the *ab initio* calculation of Czuchaj and his co-workers, nevertheless they also show a very good agreement with the latter. For the heavier RG atoms (i.e., Ar, Kr, and Xe), according to Refs. [1–3], the interatomic PE curves appear to become strongly attractive with decreasing value of R. The strength of the bonding increases rapidly while going from Ar, through Kr, to Xe. This effect is strongly supported by the experimental results of earlier studies performed in this laboratory [8]. Furthermore, according to the *ab initio* results the potential barrier becomes smaller when going in a sequence of molecules from MAr, through MKr, to MXe (M=Cd or Hg). However, the heights of the barrier decreases and converts gradually into an outer shallow minimum which eventually vanishes, reaching the dissociation limit at yet larger values of R. A similar conclusion, with respect to the shape of the $^3\Sigma^+(7\,^3S_1)$-state PE curve in HgAr, was drawn for the first time by Duval *et al.* [9,10], and it was based entirely on experimental observations and simulations of the spectra. All of the above studies reveal a real complexity of the seemingly simple nature of the vdW bonding, especially that of the excited states. The PE curve of a vdW diatom is in fact very difficult to predict because of a labile balance between the repulsive overlap forces and the multitude of attractive forces involved [11,12].

This paper reports additional results of our systematic studies which were undertaken recently in this laboratory on the CdRG complexes in their lowest Rydberg states. The first two papers were related to the CdNe [5] and CdAr [6] com-

*Email address: ufkopers@cyf-kr.edu.pl
†Email address: mczajko@uwindsor.ca
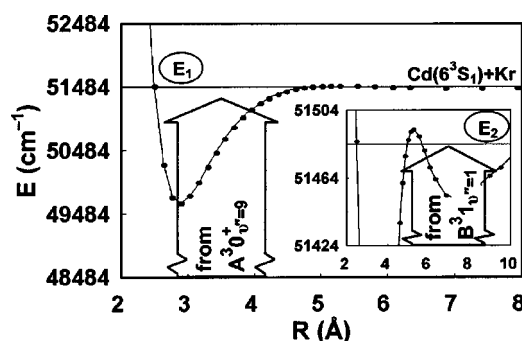
FIG. 1. Potential-energy curve of the $E\ ^3\Sigma^+(6\ ^3S_1)$ lowest Rydberg electronic state of CdKr resulting from *ab initio* calculation of Czuchaj and Stoll [1] (full circles). Wide arrows represent a range of laser excitation from the $A\ ^30^+_{v''=9}$ and $B\ ^31_{v''=1}$ intermediate states to the v' levels in the inner (E_1) and outer (E_2, see inset) wells, respectively.

plexes, while in this paper we report on the investigation of the CdKr molecule (using the OODR approach) excited to the $E\ ^3\Sigma^+$ state via two different intermediate states: $A\ ^30^+_{v''=9}[\leftarrow X\ ^10^+_{v''=0}]$ or $B\ ^31_{v''=1}^+[\leftarrow X\ ^10^+_{v''=0}]$. As a result, well-defined bound-bound and bound-free spectra were observed. Figure 1 presents the PE curve of the $E\ ^3\Sigma^+$ state in CdKr resulting from *ab initio* calculation of Czuchaj and Stoll (full circles) [1]. The wide arrow on the left-hand side indicates a range of the laser excitation to the v' levels in the inner E_1 well (for the sake of clarity we denote E_1 and E_2 as the inner and outer wells of the same $E\ ^3\Sigma^+$ electronic state, respectively). It leads to an excitation spectrum originating from the $A\ ^30^+_{v''=9}$ level. An inset in Fig. 1 shows the long-range part of the $E\ ^3\Sigma^+$-state PE curve revealing certain details, i.e., the potential barrier and outer E_2 well that may accommodate v' levels which, if excited from the $B\ ^31_{v''=1}$ level, may lead to a separate excitation spectrum. The advantage of such an exploration is evident: if we take into account that the locations of the PE minima of the two intermediates differ considerably [i.e., $R''_e(A\ ^30^+) < R''_e(B\ ^31)$ [8,13,14], the probing of the Rydberg-state potential can be performed in a more detailed way over a large interval of R. Different methods of analysis of the recorded spectra were employed in order to obtain a reliable characterization of two bound regions of the $E\ ^3\Sigma^+$-state potential-energy curve. It has to be noted at this point that the $E\ ^3\Sigma^+$ state (Hund's case a) is degenerated with respect to the values of $\Omega=1,0^-$ (Hund's case c) as shown in Refs. [1,2,10].

II. EXPERIMENT

The arrangement of the apparatus used in the OODR experiments was reported previously [5,6]. In the present paper we describe only the most important and relevant modifications which were employed in the recent studies. The CdKr molecules produced in a supersonic-expansion beam (carrier-gas mixture of 20% Kr in He, Praxair Canada Inc.) were irradiated with two successive laser pulses. The first pulse was generated with an in-house-built dye laser pumped with a second-harmonic output of Nd$^+$:YAG (yttrium aluminum
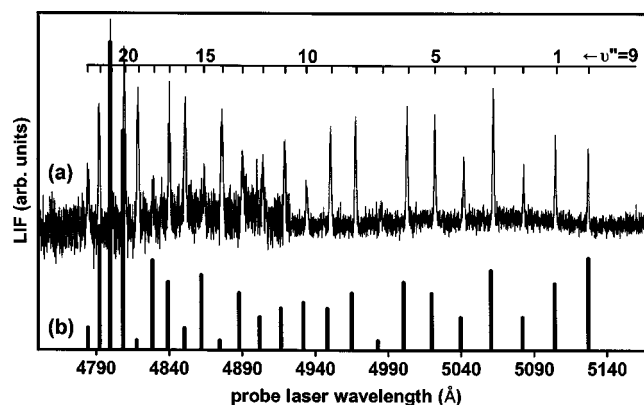
FIG. 2. (a) Excitation spectrum of the $(E_1)_{v'} \leftarrow A\ ^30^+_{v''=9}[\leftarrow X\ ^10^+_{v=0}]$ transition recorded using the optical-optical double-resonance method. (b) Calculated Franck-Condon factors for the $(E_1)_{v'} \leftarrow A\ ^30^+_{v''=9}$ progression with an assumption that both potentials are represented with Morse functions. Molecular constants (used here) are those determined in this study (Table II).

garnet) laser (YG661-10, Quantel). The dye-laser output was frequency doubled (range 3258 Å–3273 Å) to excite a maximum number of the CdKr molecules from the $X\ ^10^+_{v=0}$ ground to the $A\ ^30^+_{v''=9}$ or $B\ ^31_{v''=1}$ intermediate levels. The primarily excited molecules were irradiated with a second pulse from an in-house-built nitrogen-laser pumped dye laser (range 4790 Å–5130 Å). The second pulse excites the molecules to the v' levels in the $E\ ^3\Sigma^+$ state. A delay between the two dye-laser pulses was varied between 20 ns and 50 ns to ensure an efficient excitation in the process. The laser-induced fluorescence signal was observed perpendicular to the plane containing the molecular and laser beams and was detected with a Hamamatsu R2496 photomultiplier tube (PMT) shielded from an intense first-step excitation radiation by an UV-absorbing filter. The molecular-beam source was operated at a temperature 920 K which corresponds to the saturated Cd vapor pressure of 160 torr [15]. Further details on supersonic beam experiments can be found elsewhere [16].

III. RESULTS AND DISCUSSION

A. Excitation spectrum of the $(E_1)_{v'} \leftarrow A\ ^30^+_{v''=9}$ transition

Figure 2(a) shows the excitation spectrum recorded at the $(E_1)_{v'} \leftarrow A\ ^30^+_{v''=9}$ transition. A total of 24 vibrational components in the range 4780 Å–5140 Å were observed. As we shall see below, a further analysis will justify our *a priori* assumption that the $v'=23$ component, i.e., the apparent blue edge of the spectrum, is not yet a dissociation limit of the molecule in the $E\ ^3\Sigma^+$ state. The limitation originates rather as a result of the Franck-Condon (FC) principle in the excitation. The component of the longest wavelength observed was tentatively assigned to the $v'=0 \leftarrow v''=9$ transition. The assignment was confirmed in further analysis and simulation of the spectrum. The choice of the $v''=9$ level as the intermediate was motivated by a large FC factor for the initial $A\ ^30^+_{v''=9} \leftarrow X\ ^10^+_{v=0}$ transition [13], and hence it ensured a

high production yield of CdKr in the chosen level. The probing radiation (second laser pulse) excited the $(E_1)_{v'}$ levels which decayed to the $A\ ^3 0^+(5\ ^3P_1)$, $B\ ^31(5\ ^3P_1)$, $a\ ^30^-(5\ ^3P_0)$, $b\ ^32(5\ ^3P_2)$, $c\ ^31(5\ ^3P)$, and $d\ ^30^-(5\ ^3P_2)$ lower electronic states emitting detectable fluorescence. A large part of the bound-free decays to the repulsive part of the $X\ ^10^+$ state (after the first-excitation process) produced an UV radiation which had to be prevented from entering the PMT (see Sec. II). As seen in Fig. 2(a), the spectrum is affected by a broad, noiselike, background observed mostly between the $v'=11$ and $v'=19$ components. It seems that the inelastic collisions of the molecules in the $A\ ^3 0^+_{v''=9}$ level with He carrier-gas atoms may cause a significant population of neighboring v'' levels and consequently lead to the observed phenomenon. Indeed, a closer inspection of the components profiles suggest also a high rotational temperature in the expansion beam. The phenomenon of similar collisionally produced "ghosts" vibrational components and their relation to the parameters of expansion of the beam has been studied in detail and discussed elsewhere [6,17,18]. In our present experiment, a total of 28 vibrational components were recorded and examined to determine the $E\ ^3\Sigma^+$-state potential parameters. Some additional components were observed by probing the E_1 well from the $B\ ^31_{v''=1}$ level as presented in a discussion in Sec. III C. All wavelengths and frequencies of observed vibrational components are listed in Table I.

B. Characterization of the E_1 potential-energy well

1. The depth of the E_1 potential-energy well

We began our analysis of the spectrum shown in Fig. 2(a) with an assumption that it represents the $(E_1)_{v'}\leftarrow A\ ^30^+_{v''=9}$ progression and its first component at 5126.50 Å corresponds to the $0\leftarrow9$ transition. Applying the Birge-Sponer (BS) [19] method to the results collected in Table I we obtained a plot $[\Delta G(v'+1/2)$ against $v']$ shown in Fig. 3. A so-called "short" extrapolation of the linear part of the plot is considered a safe and reliable way to obtain the values of fundamental frequency ($\omega'_0=90.0\ \mathrm{cm}^{-1}$) and anharmonicity ($\omega'_0 x'_0 =1.25\ \mathrm{cm}^{-1}$) by means of the BS method [20]. Within the validity of this method the following approximations are allowed and used: $\omega'_0 x'_0 \approx \omega'_e x'_e$, $\omega'_e \approx \omega'_0 + \omega'_0 x'_0$. Based on these evaluations the dissociation energy of the molecule in the $E\ ^3\Sigma^+$ state of the inner well was found with a value $D'_0 =1620\ \mathrm{cm}^{-1}$. Second, a "long" extrapolation towards the $\Delta G=0$ yielded a limiting value of a vibrational quantum number $v'_D=36$. The linearity of the BS plot has been strengthened to some extent by several vibrational components recorded in the excitation spectrum of the $(E_1)_{v'} \leftarrow B\ ^31_{v''=1}$ transition (open circles in the linear plot of Fig. 3, and see also the discussion of Sec. III C). Therefore, the applicability and reliability of the BS method for the data analysis have been also strengthened. Besides the BS analysis, a LeRoy-Bernstein (LRB) method [21,22] was applied. The method and criteria of its applicability in particular cases of MRG vdW molecules (M=metal atoms of the 12th group of the periodic table of the elements) are presented in detail elsewhere [16]. A result of the LRB analysis (a dissociation

TABLE I. The wavelengths in air ($\lambda_{\mathrm{air}}\pm0.05$ Å) and frequencies *in vacuo* ($\nu_{\mathrm{vac}}\pm0.2\ \mathrm{cm}^{-1}$) of the $(E_1)_{v'}\leftarrow A\ ^30^+_{v''=9}$ transition in CdKr.

v'	λ_{air} (Å)	ν_{vac} (cm^{-1})
0	5126.50	19 501.0
1	5103.45	19 589.1
2	5081.30	19 674.5
3	5060.55	19 755.2
4	5049.00	19 835.7
5	5020.15	19 914.2
6	5001.00	19 990.4
7	4983.00	20 062.6
8	4965.30	20 134.1
9	4948.20	20 203.7
10	4931.70	20 271.3
11	4916.50	20 334.0
12	4902.25	20 393.1
13	4888.40	20 451.0
14	4874.70	20 508.3
15	4862.50	20 560.0
16	4849.60	20 610.1
17	4839.00	20 657.0
18	4829.10	20 703.0
19	4818.00	20 749.0
20	4808.20	20 791.0
21	4799.25	20 830.0
22	4791.40	20 865.0
23	4784.00	20 897.1
24	4777.10[a]	20 927.3[b]
25	4770.70[a]	20 955.3[b]
26	4765.10[a]	20 980.3[b]
27	4759.80[a]	21 003.1[b]

[a]Values corresponding to vibrational bands observed in the excitation spectrum of the $(E_1)_{v'}\leftarrow B\ ^31_{v''=1}$ transition.
[b]Frequencies obtained by adding an increment of $\Delta\nu_{(A_{v''=9}-B_{v'=1})} =152.3\ \mathrm{cm}^{-1}$ to the frequencies of the observed bands (see Sec. III C1 and Fig. 4).

limit $D_{\mathrm{diss}}=21\ 127\ \mathrm{cm}^{-1}$) is shown in the inset of Fig. 3. The D_{diss} is related directly to the $D'_0(E_1)$ [21]:

$$D'_0(E_1)=D_{\mathrm{diss}}-\nu_{09}, \qquad (1)$$

where ν_{09} is a frequency of the $0\leftarrow9$ transition from the $A\ ^30^+$ state to the E_1 well. Using $\nu_{09}=19\ 501.0\ \mathrm{cm}^{-1}$ (Table I), Eq. (1) yields $D'_0(E_1)=1627.0\ \mathrm{cm}^{-1}$, which coincides well with the result of the BS analysis. This additional processing of our results by means of the LRB method was performed for a simple reason: to test reliability of our experimental data. It seems reasonable to assume that both methods when applied, as in this case, to similar Morse's potentials involved in the spectrum producing transitions (with adequate number of vibrational components—as required by the applicability rules), they
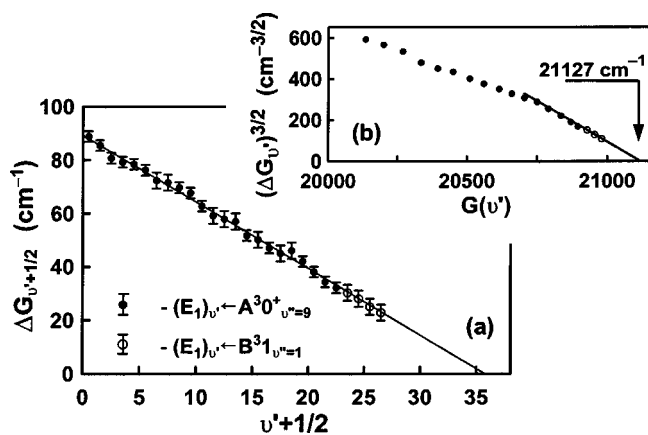
FIG. 3. Birge-Sponer plot of the v' progression recorded in the $(E_1)_{v'} \leftarrow A\,^3 0^+_{v''=9}$ (full circles) and $(E_1)_{v'} \leftarrow B\,^3 1_{v''=1}$ transitions (open circles). Insert shows LeRoy-Bernstein plot for the E_1 inner well of the $E\,^3\Sigma^+$ state. Extrapolation of the points closest to the dissociation limit determine a value of the D_{diss}. For both plots frequencies listed in Table I were used.

should reproduce the same molecular parameters within a reasonable (and tolerable) interval of deviations. Deviations or small differences in numerical estimations may be due to slight differences in interactions assumed in the application of the methods. The results seem to justify our reasoning as being evidently true in this case.

2. Simulation of the excitation spectrum of $(E_1)_{v'} \leftarrow A\,^3 0^+_{v''=9}$ transition

Molecular parameters obtained for the E_1 inner well and those for the intermediate $A\,^3 0^+$ state [13] were used to simulate the excitation spectrum of the $(E_1)_{v'} \leftarrow A\,^3 0^+_{v''=9}$ transition. It was assumed that both states are described by Morse potentials. This assumption is justified by the fact that in the present paper, as well as in Ref. [13], the BS method shows a strong linear dependency of ΔG vs v in a region of v' and v'', thus contributing to the spectrum simulated in the discussion presented here. The "best fit" was obtained using frequency of the $0 \leftarrow 0$ transition with $\nu_{00} = 19\,776.7$ cm^{-1}. ν_{00} was evaluated by adding to the observed ν_{09} a term value $G_0(v'=9) = 275.7$ cm^{-1}, which is an amount of energy compensating the difference between the vibrational levels of the initial electronic state. Figure 4 illustrates clearly rationality of this procedure. Several trials with other ν_{00} values were not successful. Therefore, we accepted the original assumption of the v' assignment. The best fit yielded also a difference of the equilibrium internuclear separation $\Delta R_e = R_e''(A\,^3 0^+) - R_e'(E_1) = 0.35 \pm 0.05$ Å. It is worthwhile to mention that a theoretical ΔR_e^{th} value ($\Delta R_e^{\text{th}} = 0.40$ Å [1]) coincides very well with the obtained result. This indicates that the minimum of the E_1 well is shifted towards shorter values of R with respect to the $A\,^3 0^+$-state PE curve. Since $R_e''(A\,0^+)$ is well known and accepted [13], therefore our result for the equilibrium internuclear separation in PE well E_1 is $R_e'(E_1) = 2.99 \pm 0.05$ Å (note again that $R_e'^{\text{th}}(E_1) = 2.91$ Å according to Ref. [1]). In Fig. 2(b) a simulated spectrum is shown and compared with the experimental results. The comparison is
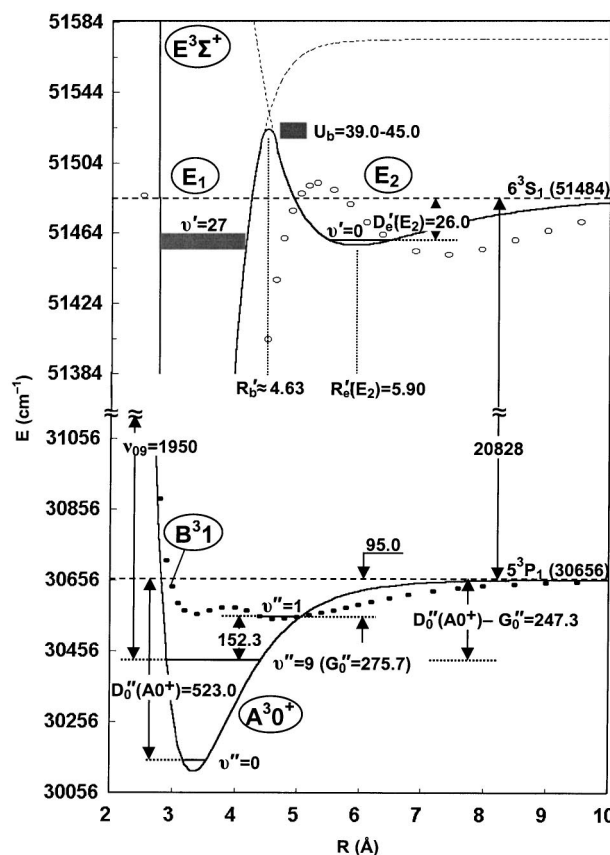
FIG. 4. Potential-energy curves of the $E\,^3\Sigma^+$ Rydberg state (solid line, this work) as well as two $A\,^3 0^+$ (solid line, [13]) and $B\,^3 1$ (full circles, [14]) intermediate states in CdKr. *Ab initio* points of Czuchaj and Stoll [1] (open circles) for the Rydberg state are also presented. Construction details of the potential barrier in the $E\,^3\Sigma^+$ state are shown (the range of U_b as well as $v'=27$ is illustrated with a horizontal bar). Values of various energy differences (in cm^{-1}) and internuclear separations (in Å) that are discussed in the text are depicted.

reasonably satisfactory. All the molecular parameters obtained as a result of this study are summarized in Table II.

3. Potential barrier in the $E\,^3\Sigma^+$ state

Existence of a potential barrier and its experimental proof seem to be an important question in view of the results of *ab initio* calculations [1,2]. We approached the problem by estimating the depth of the E_1 well using our experimental results as well as the appropriate atomic values generally accepted in atomic spectroscopy [23]. First, we evaluated the $D_0'(E_1)$ by employing the atomic [23] and molecular [13] data as well as different methods of analysis. Using $\nu_{00}(E_1 \leftarrow A\,^3 0^+)$ and values of the $A\,^3 0^+$-state potential parameters we calculated vibrational term $G_0(v'')$ [24],

$$G_0(v'') = \omega_0 v'' - \omega_0 x_0 v''^2, \qquad (2)$$

and for $v'=9$ obtained $G_0(v'=9) = 275.7$ cm^{-1}. Employing atomic data of Ref. [23], we arrived at

TABLE II. Potential parameters of CdKr in the $X\,^1 0^+$, $B\,^3 1$, $A\,^3 0^+$, $C\,^1 1$ and $E\,^3\Sigma^+$ (inner well, E_1) molecular states. All in cm^{-1} unless stated otherwise. Note $\Delta R_e = R_e'' - R_e'$.

	$X\,^1 0^+(^1\Sigma^+)$	$A\,^3 0^+(^3\Pi)$	$B\,^3 1(^3\Sigma^+)$	$C\,^1 1(^1\Pi)$	$E\,^3\Sigma^+$ (inner well)
ω_0	17.6[a]	36.3[a]	9.1[b]	58.0[a]	90.0±1.0[c]
ω_e	18.1[a]	37.0[a]	9.3[a]	58.9[a]	91.0±1.0[c]
	15.3[d]	36.1[d]	9.2[d]	48.8[d]	
$\omega_e x_e$	0.50[a]	0.63[a]	0.20[a]	0.85[a]	1.25±0.01[c]
D_0	155.0[a]	523.0[a]	104.0[a]	1060.0[a]	1620.0±6.0[c]
					1627.0±8.0[e]
D_e	165.0[a]	541.0[a]	112.0[a]	1090.0[a]	1656.0±3.0[c]
	134.0[d]	535.0[d]	109.2[b]	843.0[d]	1837[d]
			112.0[d]		
ΔR_e(Å)		0.93[a]	−0.51[b]	1.165[a]	0.35±0.05[f]
					0.39[d]
R_e(Å)	4.27[a]	3.34[a]	4.97[a]	3.10[a]	2.99±0.05[f]
	4.45[d]	3.39[d]	4.70[b]	3.13[d]	2.91[d]
			4.97[d]		
ν_{00}		30 287.0[a]	30 706.1[b]	42 787.0[a]	19 776.7±2.0[f]
ν_D	18[a]	29[a]	23[b]	35[a]	36[c]
					42[h]
D_{diss}		30 811.0[a]	30 811.0[b]	43 847.0[a]	2112.7±6.0[h]
C_6(cm^{-1} Å^6)	1.2×10^6	1.5×10^6	1.7×10^6	2.45×10^6	

[a]Reference [13].
[b]Reference [14].
[c]This work, BS plot.
[d]*Ab initio* calculation, Ref. [1].
[e]This work, Eq. (1).
[f]This work, simulation of the $(E_1)_{v'} \leftarrow A\,^3 0^+_{v''=9}$ spectrum.
[g]This work, $\nu_{00} = \nu_{09} + G_0(v''=9)$ [see Eq. (2)].
[h]This work, LRB analysis.

$$\Delta\nu_{\mathrm{at}} = \nu_{\mathrm{at}}(6\,^3 S_1) - \nu_{\mathrm{at}}(5\,^3 P_1) = 20\,828.0\ \mathrm{cm}^{-1}. \quad (3)$$

From the relationship

$$\Delta\nu_{\mathrm{at}} + D_0''(A\,^3 0^+) - G_0(v''=9) = \nu_{09} + D_0'(E_1), \quad (4)$$

where ν_{09} and $D_0''(A\,^3 0^+)$ were taken from Table I and from Ref. [13], respectively, we *estimated* dissociation energy $D_0'(E_1)_{\mathrm{estim}} = 1574.3 \pm 10.0$ cm^{-1}. As it has been already mentioned, using BS plot (Fig. 3) we obtained $D_0'(E_1)_{\mathrm{BS}} = 1620.0 \pm 6.0$ cm^{-1} while from LRB analysis [an inset in Fig. 3 and Eq. (1)] a value of D_{diss} leads to $D_0'(E_1)_{\mathrm{LRB}} = 1627.0 \pm 8.0$ cm^{-1}.

It has to be stressed that $D_0'(E_1)_{\mathrm{estim}}$ is obtained on the basis of well-accepted atomic and molecular data, and we have *also silently assumed* that the dissociation limit of the E_1 PE well coincides with the $6\,^3 S_1$ atomic asymptote. We expect that in this particular case the estimated energy should be the same as that obtained from molecular spectra. On the other hand, the BS as well as LRB methods lead to values of $D_0'(E_1)$ as an energy defined from the $v'=0$ vibrational level up to the dissociation limit. It totally disregards a configuration or a shape of the $E\,^3\Sigma^+$-state PE curve which *may appear* as a smooth molecular-to-atomic-asymptote curve or *it pear* as a smooth molecular-to-atomic-asymptote curve or *it*

may approach (with its long-range branch) a top of the barrier separating the inner well from another, e.g., outer well E_2 as shown in Fig. 1 (see the inset) and also in Fig. 4. In the latter case such an energy *may* differ from the *estimated one*. As seen from the numerical evaluations above, the estimated dissociation energy differs considerably from that obtained from the BS and/or LRB plots. The difference amounts from 45 cm^{-1} to 51 cm^{-1} above the atomic Cd($6\,^3 S_1$) asymptote. We assigned this difference to the existence of a positive barrier as predicted in Refs. [1,2]. There is however a second way (which should be explored for the sake of the reliability of the estimation method) to define and ultimately to estimate the numerical value of the barrier. For example, Eq. (3) describes the dissociation limit at the atomic asymptote as the $\Delta\nu_{\mathrm{at}}$. The same energy difference can be expressed using experimentally evaluated molecular parameters $\Delta\tilde{\nu}_{\mathrm{at}} = \nu_{09} - [D_0''(A\,^3 0^+) - G_0(v''=9)] + D_0'(E_1)_{\mathrm{BS}} = 20\,873.7$ cm^{-1}. Obviously, $\Delta\tilde{\nu}_{\mathrm{at}} > \Delta\nu_{\mathrm{at}}$ therefore, we defined $U_b = \Delta\tilde{\nu}_{\mathrm{at}} - \Delta\nu_{\mathrm{at}}$ as the height of the barrier in the $E\,^3\Sigma^+$ state. U_b is measured from the $6\,^3 S_1$ atomic asymptote (see Fig. 4) and numerically $U_b = 45 \pm 10$ cm^{-1}. In the following section we shall discuss an excitation spectrum originated from the other (i.e., $B\,^3 1$) intermediate state. Its interpretation leads to a height of the barrier as 40 cm$^{-1} \leqslant U_b \leqslant 45$ cm^{-1}. On the other hand,
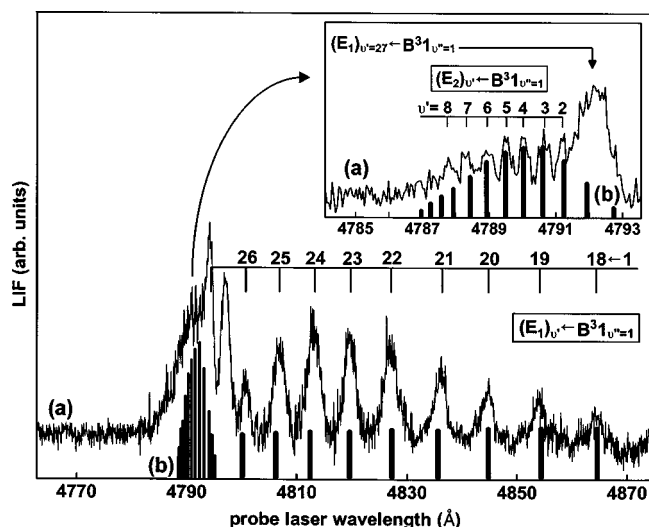
FIG. 5. (a) Excitation spectrum of the $E_{v'} \leftarrow B \, ^3 1_{v''=1}$ $[\leftarrow X \, ^1 0^+_{v=0}]$ transition obtained by means of the optical-optical double-resonance method. The spectrum consists of two v' progressions: $(E_1)_{v'} \leftarrow B \, ^3 1_{v''=1}$ and $(E_2)_{v'} \leftarrow B \, ^3 1_{v''=1}$ (see also inset). (b) Franck-Condon factors calculated for the two v' progressions based on an assumption that all potentials are represented with Morse functions using constants determined in this study (Tables II and IV).

the *ab initio* calculations [1,2] yield a considerably smaller positive value of the barrier with $U^{th}_b \approx 9$ cm^{-1}. Consequently, based on our study we may draw a conclusion that an existence of the positive barrier in the PE curve of the $E \, ^3\Sigma^+$ state has been *qualitatively* confirmed.

C. Excitation spectrum of the $E_{v'} \leftarrow B \, ^3 1_{v''=1}$ transition

In order to gain more information about the structure of the $E \, ^3\Sigma^+$-state PE curve we also probed the excited state using the $B \, ^3 1_{v''=1}$ as an intermediate. The $E_{v'} \leftarrow B \, ^3 1_{v''=1}$ excitation provides an opportunity to observe different features in the $E \, ^3\Sigma^+$-state potential otherwise not possible to detect in the former exploration. Indeed, the large internuclear equilibrium separation of $R''_e(B \, ^3 1) = 4.97$ Å [14] makes the $B \, ^3 1$-state PE curve flat and long ranging as it is seen in Fig. 4 represented by full circles. The FC overlap of the $B \, ^3 1$ and theoretically predicted $E \, ^3\Sigma^+$ [1,2] states provided an opportunity for an exploration of the Rydberg state in a wider range of R values. An excitation spectrum from the $B \, ^3 1_{v''=1}$ is shown in Fig. 5(a). Observed vibrational bands result from the $(E_1)_{v'} \leftarrow B \, ^3 1_{v''=1}$ transition and all of them can also be assigned to the vibrational bands of the $(E_1)_{v'} \leftarrow A \, ^3 0^+_{v''=9}$ transition shown in Fig. 2(a). The assignment can be performed by adding to each of the $\nu_{v',v''=1}$ frequencies recorded at the $(E_1)_{v'} \leftarrow B \, ^3 1_{v''=1}$ transition a difference of $\Delta\nu_{(A_{v''=9} - B_{v''=1})} = 152.3$ cm^{-1} as shown in Fig. 4 and in a footnote of Table I. Therefore, probing of the $E \, ^3\Sigma^+$ state via the $B \, ^3 1$ state yields four additional vibrational bands which belong to the E_1 inner well. Those additional frequencies (see Table I) improved the accuracy of the BS and LRB analyses (see Fig. 3) and, hence, the accuracy of the final molecular

TABLE III. The wavelengths in air ($\lambda_{air} \pm 0.05$ Å) and frequencies *in vacuo* ($\nu_{vac} \pm 0.2$ cm^{-1}) of the $(E_2)_{v'} \leftarrow B \, 1_{v''=1}$ transition in CdKr.

v'	λ_{air} (Å)	ν_{vac} (cm^{-1})
0	4792.80	20 858.9
1	4791.95	20 862.6
2	4791.15	20 866.0
3	4790.45	20 869.0
4	4789.85	20 871.6
5	4789.35	20 873.9
6	4788.90	20 875.9

parameters. A spectrum shown in Fig. 5(a) spans a spectral range of approximately ≈ 100 Å (4770 Å–4870 Å) and it ends at the blue side with a distinctive structured "head" that appears to be wider than the rest of the spectral components (see inset in Fig. 5). The spectrum can be explained with the help of PE curves drawn in Fig. 4. Due to the restriction of the FC principle, the highest vibrational level observed in the E_1 well is that with $v' = 23$. It can be seen (as suggested in Fig. 4) that when the excitation process starts from $B \, ^3 1_{v''=1}$, the feasibility of excitation of higher levels in the E_1 well may increase and ultimately a level as high as $v' = 27$ can be excited. When the probe-laser frequency reaches the limiting value and excites the vibronic level with $v' = 27$ in the E_1 well, it also enters simultaneously into the region of a bound-free excitation. This phenomenon has been also previously observed in the analogous CdNe and CdAr spectra [5,6]. Indeed, the shape of the wide band, divided by a very sharp dip between $v' = 26$ and $v' = 27$, shows distinctly what can be interpreted as the Condon internal diffraction pattern in excitation. It is commonly understood as a projection of a vibrational wave function of the $v'' = 1$ level onto a repulsive part of the $E \, ^3\Sigma^+$-state PE curve in the region of the E_1 well. It results as a spectral trace of a continuum with characteristic undulatory nodal structure [4–7]. However, the probe-laser frequency can also excite the densely spaced vibrational levels in the E_2 outer well. These two effects contribute eventually to a final shape of the observed band. In the analysis of the spectrum, this new structure was indeed identified as series of vibrational bands (see Table III for their frequencies) belonging to the outer well theoretically predicted. Figure 6 shows the BS plot, while the inset presents a result of the LRB analysis. Both procedures lead to nearly the same value of $D'_0(E_2)$-dissociation energy and yield a set of spectroscopical parameters for the E_2 well (see Table IV). Using these parameters and those of Table II, we were able to simulate both $(E_1)_{v'} \leftarrow B \, ^3 1_{v''=1}$ and the $(E_2)_{v'} \leftarrow B \, ^3 1_{v''=1}$ excitation spectra. The result of the simulation is shown in Fig. 5(b). In the simulation, Morse representations were assumed for both (intermediate and Rydberg states) potentials as it is well justified for all PE curves presented in this work. The simulation seems to represent all the experimental spectral traces in a satisfactory way.
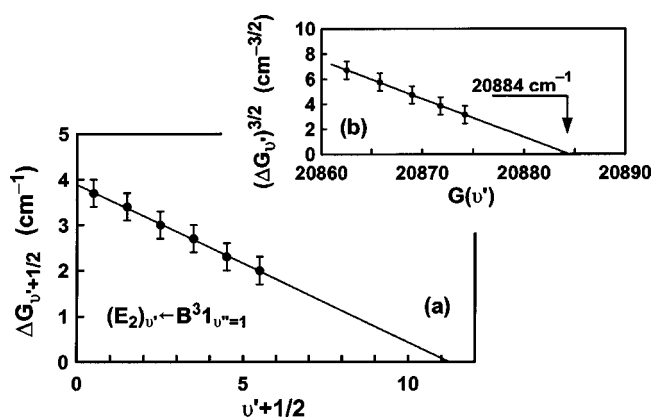
FIG. 6. Birge-Sponer plot of the v' progression of the $(E_2)_{v'}$ $\leftarrow B\ ^31_{v''=1}$ transition. Inset shows LeRoy-Bernstein plot for the outer well of the $E\ ^3\Sigma^+$ state. For both plots frequencies listed in Table III were used.

D. Comparison with results of *ab initio* calculations

The simulation procedure described in Sec. III C1 generated the value of $R'_e(E_2)=5.90\pm0.05$ Å for the location of the minimum equilibrium separation within the outer PE well. In Fig. 4 this result is compared with that of Czuchaj and Stoll

TABLE IV. Potential parameters of CdKr in the $E\ ^3\Sigma^+$ molecular state (outer well, E_2). All in cm^{-1} unless stated otherwise. Note $\Delta R_e = R''_e - R'_e$.

	$E\ ^3\Sigma^+$ (outer well)[a]
ω'_0	3.9 ± 0.15[a]
ω'_e	4.1 ± 0.15[a]
$\omega'_e x'_e$	0.170 ± 0.008[a]
D'_0	22.4 ± 2.0[a]
	25.0 ± 2.0[b]
D'_e	25.0 ± 2.0[a]
	27.0 ± 2.0[b]
	32.4[c]
$\Delta R'_e$ (Å)	-1.10 ± 0.05[d]
	-2.38[c]
R'_e (Å)	5.90 ± 0.05[d]
	7.40[c]
$\nu_{0v''}$	20858.9 ± 2.0[e]
	$20\,868.0\pm2.0$[f]
v'_D	11.5[a]
	15[b]
D'_{diss}	$20\,884.0\pm2.0$[b,e]
	$20\,893.0\pm2.0$[f]
C'_6 (cm^{-1} Å^6)	11.3×0^6[b]

[a]This work, BS plot.
[b]This work, LRB analysis.
[c]*Ab initio* calculation, Ref. [1].
[d]This work simulation of the $(E_2)_{v'} \leftarrow B\ ^31_{v''=1}$ spectrum.
[e]This work, defined from $B\ ^31_{v''=1}$.
[f]This work, defined from $B\ ^31_{v''=0}$.

and is indicated by open circles [1]. The experimental depth of the E_2 well, $D'_e(E_2)=27$ cm^{-1}, is comparable with the result of Ref. [1] which yields $D'^{th}_e(E_2)=32.4$ cm^{-1}, but the value of $R'_e(E_2)$ shows a striking difference with respect to the theoretical value $R'^{th}_e(E_2)=7.4$ Å [1]. Indeed, it is rather difficult to imagine (in our opinion) vibrational transitions (obeying the FC principle with adequate transition probabilities) launched from the $B\ ^31_{v''=1}$, to v' levels of the E_2 well at this particular shape of PE curve with the value of $R'^{th}_e(E_2)$ as calculated. Obviously, the location of the E_2 PE well may have an influence on the position of the barrier in the $E\ ^3\Sigma^+$ state. An estimation of this work locates the barrier at $R'_b \approx 4.63$ Å which should be compared with theoretical $R'^{th}_b =5.03$ Å [1].

E. Remarks on the $E\ ^3\Sigma^+$ Rydberg-state potential

The PE curve of the Rydberg $E\ ^3\Sigma^+$ state shown in Fig. 4 was constructed using two Morse representations following the construction method suggested in Ref. [7] and in some recent studies reported from this laboratory [5,6]. We also employed all experimental parameters of the E_1 and E_2 potential wells presented in Tables II and IV of this paper. The double-well potential suggestion seems to be a rational representation of the $E\ ^3\Sigma^+$ state. It means that at long distance, e.g., at $R>4.60$ Å, a weakly bound vdW complex is formed as a result of a dispersion interaction between the Cd($6\ ^3S_1$) and Kr atoms (see discussion in Ref. [16]). It is reasonable to assume that the $6s$ orbital of a Rydberg electron extends out as far as it is able to initiate a repulsion of the electronic cloud which hinders the approach of Kr atom at a distance that eventually leads to an equilibrium at $R'_e=5.90$ Å and a barrier at a distance of approximately $R_b=5.6$ Å. On the other hand the reports of authors on HgAr molecule in its Rydberg state [4,7,9,10] are consistent with explanation regarding the origin of the inner PE well. They assumed that it should be attributed to the attraction between the Hg-Ar$^+$ ionic core (presumably a *charge-charge-induced dipole interaction*) and the $7s$ electron mostly outside the Ar atom. A general similarity between the ground-state CdKr studied here and the case of HgAr molecule may lead to some speculations about a similarity of interaction in the excited states. As an example, to some extent justifying such speculations, we summarized (Table V) the main molecular parameters of two types of vdW molecules: CdNe, CdAr, CdKr, and HgNe as well as HgAr in their lowest Rydberg states. The first three molecules have been investigated in our laboratory [5,6], while the last two have been reported elsewhere [4,7,9,10]. The regularities in numerical behavior of the molecular parameters of these two families of molecules seem to be striking, but we are convinced that this is all we can say at this point and that no more speculations should and can be allowed, nor drawn at the present level of our knowledge about the CdKr cluster. We do not have unfortunately any stronger arguments at this time but we tend to believe that the attraction within the E_1 well in CdKr molecule may indeed correspond to that of a Cd-Kr$^+$ ionic core system with the $6s$ electron mostly outside the Kr atom as suggested for HgAr. Therefore, the interatomic potential of the Rydberg state, if

TABLE V. Potential parameters of CdNe, CdAr and CdKr ($n=6$) as well as HgNe and HgAr ($n=7$) molecules in the $E\,^3\Sigma^+(n\,^3S_1)$ electronic energy states. Note E_1, inner well, and E_2, outer well.

| Designation | CdRG[a] | | | | | | HgRG[b] | | | |
| | CdNe | | CdAr | | CdKr | | HgNe | | HgAr | |
	E_1	E_2	E_1	E_2	E_1	E_2	E_1	E_2	E_1	E_2
ω_e (cm^{-1})	56.6		107.1	4.4	91.0	4.1	61.6		112.0	4.3
$\omega_e x_e$ (cm^{-1})	8.8		2.1	0.20	9.6	0.17	9.6		2.01	0.17
D_e (cm^{-1})	91.0		1309.5	24.2	1656.0	27.0	98.8		1460.0	38.0
E_b (cm^{-1})	132.1		48.0		40.0		153.0		22.0	
R_e (Å)	3.21		2.85	5.6	2.99	5.90	3.10		2.81	6.95

[a]This work and Refs. [5,6].
[b]References [4,7,9,10].

expressed analytically, should be divided, as is suggested in Ref. [4], into two parts: one part (E_1) which represents the ionic-core charge-charge-induced dipole attraction and a second part (E_2) which originates from the dispersive forces of the outer 6s electron of Cd and 4s electron shell of Kr. A position of the potential barrier should be related to the most outer maximum of the 6s Rydberg orbital wave function.

IV. CONCLUSIONS

Excitation spectra of the $E_1 \leftarrow A\,^30^+_{v''=9}$, $E_1 \leftarrow B\,^31_{v''=1}$ and $E_2 \leftarrow B\,^31_{v''=1}$ transitions in CdKr van der Waals molecule were recorded using an optical-optical double-resonance method. The $E\,^3\Sigma^+$ lowest Rydberg state was reached via two different intermediate states, $A\,^30^+$ and $B\,^31$, primarily excited from the ground $X\,^10^+$ state. By choosing an excitation from different intermediates, a more detailed way of probing and exploring the Rydberg-state interatomic potential at relatively large internuclear separation R was achieved. Two kinds, i.e., bound-bound and bound-free excitation spectra were recorded. Various analyses as well as simulations of the bound-bound spectra proved that the PE curve of the $E\,^3\Sigma^+$ state has a double-well structure. Characteristics of both potential wells have been determined and compared with results of *ab initio* calculations [1,2]. A reasonable overall agreement of the experimental results and theoretical predictions is evident. Following the discussion on the HgAr complex in its $^3\Sigma^+$ Rydberg state [4,7,9,10] and due to its general resemblance to the $E\,^3\Sigma^+$ state in CdKr molecule studied here, a shape of the Rydberg-state PE curve was explained on the basis of two types of interaction: long-range van der Waals (forming a weak bond) and short ranged of the ionic character (Cd-Kr$^+$) as charge-charge-induced dipole attraction which manifests itself by a relatively strong bond.

[1] E. Czuchaj and H. Stoll, Chem. Phys. **248**, 1 (1999).
[2] E. Czuchaj, M. Krośnicki, and H. Stoll, Theor. Chem. Acc. **105**, 219 (2001).
[3] E. Czuchaj, M. Krośnicki, and H. Stoll, Chem. Phys. **263**, 7 (2001).
[4] M. Okunishi, K. Yamnaouchi, K. Onda, and S. Tsutchiya, J. Chem. Phys. **98**, 2675 (1993).
[5] J. Koperski and M. Czajkowski, Chem. Phys. Lett. **357**, 119 (2002).
[6] J. Koperski and M. Czajkowski, Spectrochim. Acta, Part A **59**, 2435 (2003).
[7] K. Onda, K. Yamanouchi, M. Okunishi, and S. Tsuchiya, J. Chem. Phys. **101**, 7290 (1994).
[8] M. Czajkowski, R. Bobkowski, and L. Krause, Phys. Rev. A **45**, 6451 (1992).
[9] W. H. Breckenridge, M. C. Duval, C. Jouvet, and B. Soep, Chem. Phys. Lett. **122**, 181 (1985).
[10] M. C. Duval, O. Benoist D'Azy, W. H. Breckenridge, C. Jouvet, and B. Soep, J. Chem. Phys. **85**, 6324 (1986).
[11] F. London, Z. Phys. Chem. Abt. B **11**, 222 (1930).
[12] B. L. Blancy and G. E. Ewing, Annu. Rev. Phys. Chem. **27**, 559 (1976).
[13] J. Koperski, M. Łukomski, and M. Czajkowski, Spectrochim. Acta, Part A **58**, 2709 (2002).
[14] M. Łukomski, J. Koperski, and M. Czajkowski, Spectrochim. Acta, Part A **58**, 1757 (2002).
[15] A. Nesmeyanov, *Vapor Pressures of the Elements* (Academic Press, New York, 1963).
[16] J. Koperski, Phys. Rep. **369**, 177 (2002).
[17] D. M. Lubman, C. T. Rettner, and R. N. Zare, J. Phys. Chem. **86**, 1129 (1982).
[18] M. Czajkowski, R. Bobkowski, and L. Krause, Phys. Rev. A

41, 277 (1990).

[19] R. T. Birge and H. Sponer, Phys. Rev. **28**, 259 (1926).

[20] A. G. Gaydon, *Dissociation Energies* (Chapman and Hall, London, 1968).

[21] R. J. LeRoy and R. B. Bernstein, J. Chem. Phys. **52**, 3869 (1970).

[22] R. J. LeRoy and R. B. Bernstein, J. Mol. Spectrosc. **37**, 109

(1971).

[23] *Atomic Energy Levels*, edited by C. E. Moore, Natl. Bur. Stand. Ref. Data Ser., Natl. Bur. Stand. (U.S.) Circ. No. 35 (U.S. GPO, Washington, D.C., 1971).

[24] G. Herzberg, *Molecular Spectra and Molecular Structure. I. Spectra of Diatomic Molecules* (Van Nostrand, Princeton, 1950).